Entanglements in Linear Polystyrenes

Hiroshi Watanabe, Takashi Sakamoto, and Tadao Kotaka*

Department of Macromolecular Science, Faculty of Science, Osaka University, Toyonaka, Osaka 560, Japan. *Received November 21, 1984*

ABSTRACT: Linear viscoelastic properties were examined on binary blends of monodisperse polystyrenes (PS) having extremely short 1-chains and relatively long 2-chains (respectively with weight-average molecular weights M_{w1} and M_{w2}) to clarify the concept of entanglement. For *dilute* blends, in which 2-chains were not entangled with one another, the longest relaxation time was proportional to $M_{w1}^3 M_{w2}^2$ for blends with M_{w1} larger than the molecular weight between entanglements $M_e°$ and to $M_{w1}^0 M_{w2}^2$ for blends with $M_{w1} < M_e°$. For *concentrated* blends, in which 2-chains were entangled with themselves, the 2-chains in blends with $M_{w1} < M_e°$ behaved, at any frequency, as if they were in the solution, while for blends with $M_{w1} > M_e°$ this solution-like behavior was observed only in the low-frequency terminal zone. These results indicate that 2-chains in dilute blends with $M_{w1} > M_e°$ relax by tube renewal completely, while in concentrated blends they relax by tube renewal only partially. On the other hand, in either dilute or concentrated blends with $M_{w1} < M_e°$ 1-chains do not constrain 2-chains at all. On the basis of these experimental results and the tube model, we conclude that at the onset of entanglement in monodisperse PS, the actual relaxation mode may change from the Rouse-like mode, resulting from a (virtual) very rapid tube renewal, to the reptation-like mode, presumably influenced by a partial tube renewal process.

Introduction

The effect of entanglements on the viscoelastic properties of flexible polymers of various topology is one of the central problems in polymer rheology. Extensive experimental data on narrow molecular weight distribution (MWD) linear polymers have already been compiled,[1,2] while those on star-shaped[3-7] and H-form[8] polymers are still being compiled. A number of attempts have been made to interpret the entanglement effect in molecular terms.[1,2,9-17]

Among these theories, the Doi–Edwards theory,[11-13] based on the tube model of de Gennes,[9,10] appears to be the most intriguing one in the sense that it provides perhaps the simplest molecular picture of what would occur in entangled systems of not only linear but also star-shaped[16,17] and H-form polymers. The Doi–Edwards theory and its versions tell us that a variety of relaxation modes are possible: for monodisperse linear polymers, the relaxation modes are *reptation* without[11,12] and with contour-length fluctuation[13,14] and tube renewal;[14,15] for star-shaped and H-form chains, an additional mode is *path breathing* of a tethered (or anchored) chain.[14,16,17] For identifying these various relaxation modes experimentally, it is convenient to study the viscoelastic properties of binary blends of various types.[18-23]

Studying binary blends of poly(styrene-*b*-butadiene) diblock copolymer and polybutadiene, we identified two relaxation modes: (i) path breathing of a block polybutadiene chain with one end fixed (an anchored chain) on a polystyrene microdomain and (ii) renewal of the tube consisting of homopolybutadiene chains confining the block polybutadiene chain.[18] The former mode should be identical with the mode observed in star-shaped polymers.

We also examined the viscoelastic properties of binary blends of narrow MWD linear polystyrenes (PS) with low and high (weight average) molecular weights M_{w1} and M_{w2} (hereafter designated as 1- and 2-chains, respectively) and obtained the following results.[21,22]

For binary blends of PS with M_{w2} at least 10 times larger than M_{w1}, which was in turn larger than the molecular weight between entanglements $M_e°$ ($\cong 18 \times 10^3$) for bulk PS,[1,2] we could define a critical value w_c for the content w_2 of the 2-chain at which the behavior of the blends changes its molecular weight dependence. At w_c, the reduced molecular weight $w_2 M_{w2}$ of the 2-chain almost agreed with the characteristic molecular weight $M_c°$ ($\cong 31 \times 10^3$) for narrow MWD PS in bulk,[12] indicating that w_c corresponds to the onset of entanglement of the 2-chains with themselves. We called the blends either *dilute* or *concentrated*, according to whether w_2 was below or above w_c, respectively.[21,22]

In *dilute* blends, relaxation of 1-chains took place first, after which 2-chains entangled only with 1-chains relaxed. The longest relaxation time τ_m and the intensity P_m of the relaxation spectrum at τ_m for blends with $w_2 < w_c$ and $M_{w2}/8 > M_{w1} > M_e°$ were

$$\tau_m \propto w_2^0 M_{w1}^3 M_{w2}^2 \tag{1a}$$

$$P_m \propto w_2^1 M_{w1}^0 M_{w2}^{-1} \tag{1b}$$

In *concentrated* blends, relaxation of 1–2 entanglements appeared at intermediate times, after which relaxation of 2–2 entanglements took place. The τ_m and P_m for such blends with $w_2 \gg w_c$ and $M_{w2}/8 > M_{w1} > M_e°$ were

$$\tau_m \propto w_2^{1.5} M_{w1}^0 M_{w2}^{3.5} \tag{2a}$$

$$P_m \propto w_2^2 M_{w1}^0 M_{w2}^0 \tag{2b}$$

On the other hand, for blends with M_{w2} close to M_{w1} ($>M_e°$), the relaxation modes changed strikingly, although there was a relatively large crossover region of the M_{w2}/M_{w1} ratio (perhaps $2 < M_{w2}/M_{w1} < 8$) for this change. The asymptotic forms of τ_m and P_m in the limit $M_{w2} \to M_{w1} > M_e°$ were given, regardless of w_2, by

$$\tau_m \propto w_2^0 M_{w1}^0 M_{w2}^{3.5} \tag{3a}$$

$$P_m \propto w_2^1 M_{w1}^0 M_{w2}^0 \tag{3b}$$

We interpreted these results on the basis of the tube model and proposed the following molecular picture.[21,22]

In blends with $M_{w2} \gg M_{w1} > M_e°$, the topological constraints due to 1-chains imposed on a 2-chain become ineffective upon completion of renewal of the tube (composed of 1-chains). In *dilute* blends, 2-chains entangle only with 1-chains and, thus, relax completely by tube renewal. The results of eq 1 agree with those predicted by Klein[15] and Graessley.[14] In *concentrated* blends, however, 2–2 entanglements remain effective even after the tube composed of 1-chains has been renewed. The 2-chain must escape from the tube composed of other 2-chains by its own reptation to relax completely. Equation 2 satisfies this picture.

0024-9297/85/2218-1436$01.50/0

Table I
Characteristics of PS samples

code	$10^{-3}M_w$	M_w/M_n
L5[a]	5.2	1.08
L10[a]	10.5	1.08
L22	23.4	1.07
L36	38.9	1.07
L68	72.4	1.06
L83[a]	88.5	1.07
L118[a]	124	1.05
L161[a]	172	1.07
L294[a]	315	1.07
L407[a]	427	1.05
L1070	1190	1.11
L2580[a]	2810	1.09

[a] Supplied by Toyo Soda Mfg. Co. Ltd.

In blends with M_{w2} close to M_{w1}, the constraints due to 1-chains (on 2-chains) would survive even at long times. The 2-chains do not recognize that they are blended with 1-chains. This picture leads to eq 3.

Recently, Montfort and co-workers[23] examined binary blends of narrow MWD PS and reached essentially the same conclusions as ours, although they did not refer to the intensity P_m.

The viscoelastic functions of condensed linear polymer systems can be described essentially by two parameters: the monomeric friction coefficient ζ_0 and the molecular weight M_e between entanglements. The former defines the location of the viscoelastic functions along the time or frequency scale, while the latter determines their shape as a function of M/M_e, characterizing the effects of entanglement. For solutions, M_e is defined as a function of polymer concentration. (For bulk polymers, M_e is written as $M_e°$ for convenience.)

The tube model introduced the parameters ζ_0 and M_e, especially the latter, as ad hoc parameters but did not tell us their molecular meaning, although some attempts to solve these problems have been made.[24,25]

Thus, we extended our study on binary blends of narrow MWD PS to those with 1-chains of very low M_{w1} ($<M_e°$) to interpret the meaning of the onset of entanglement in narrow MWD polymers. In this paper, we present the results of these investigations.

Experimental Section

Anionically polymerized narrow MWD polystyrene (PS) samples were used. For convenience, hereafter we call such samples "monodisperse". The characterization of these samples was carried out by gel permeation chromatography. The details were described previously.[21,22] Table I summarizes the codes and characteristics of the samples used in this study.

To prepare test blends, prescribed amounts of the two PS samples were dissolved in benzene to make a 5 wt % solution, which was freeze-dried for 12 h at room temperature and further dried at ~80 °C under vacuum for 24 h. The dried blend was then molded at ~170 °C with a laboratory hot press into disks of a suitable size to fit the rheometer assembly.

Dynamic measurements were carried out on these disk samples at several temperatures between 95 and 240 °C with a conventional cone-and-plate rheometer (autoviscometer L-III, Iwamoto Seisakusho, Kyoto). Two sets of the cone-and-plate assembly were used. The radius of the cone and the gap angle were 15.0 mm and 3.68° and 10.0 mm and 3.49°, respectively. The storage G' and loss G'' moduli were determined by the Markovitz equation[26] without difficulty as long as $10 < [G'^2 + G''^2]^{1/2}$ (in dyn cm^{-2}) $< 10^7$ and $0.01 < G'/G'' < 100$. The time–temperature superposition principle[1] was applicable.

Results and Discussion

I. Dilute Blends. Figures 1 and 2 show the master curves of storage G' and loss G'' moduli, respectively, obtained for blends consisting of 1 wt % L2580 as the 2-chain and 1-chains with $M_{w2}/M_{w1} > 20$. All G' and G'' data are compared at an iso-free-volume state with the free volume fraction $f_r = 0.0644$.

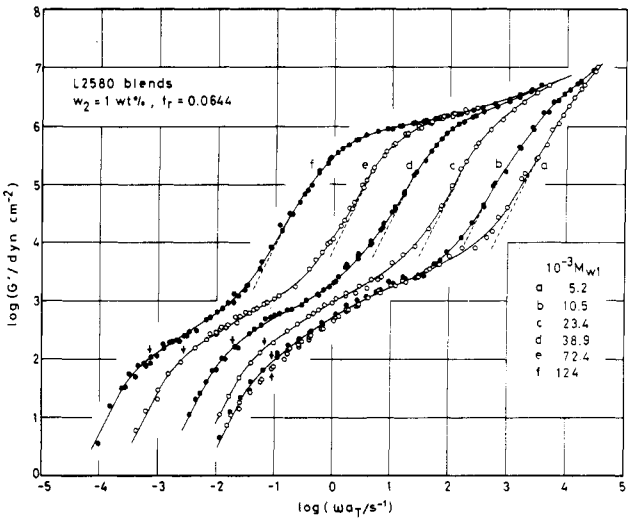

Figure 1. Master curves of the stroage moduli G' of the L2580 blends reduced at T_r where $f_r = 0.0644$. The content w_2 of L2580 in the blends is 1 wt %, and $10^{-3}M_{w1} = 5.2$, 10.5, 23.4, 38.9, 72.4, and 124 from right to left. The dashed curves are for those of the low molecular weight PS chains (1-chains). The arrows indicate the characteristic times determined by eq 6.

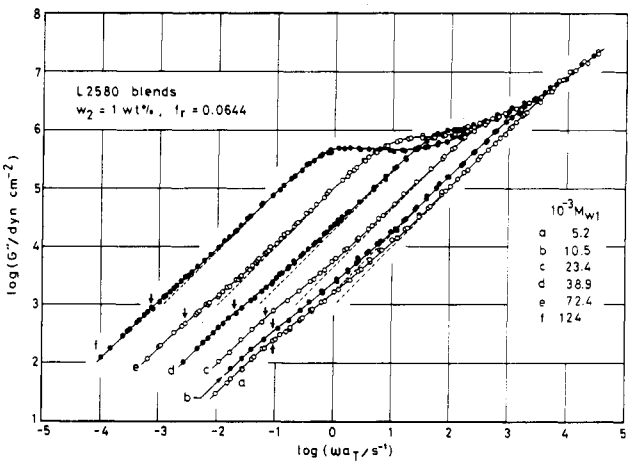

Figure 2. Master curves of the loss moduli G'' of the same L2580 blends shown in Figure 1.

Since the critical content w_c (dependent only on M_{w2}) was between 1 and 2 wt % for these L2580 blends,[21] the 1 wt % L2580 blends may be classified as *dilute* blends.

As seen in Figures 1 and 2, the master curves at high frequencies are the same as those of the constituent 1-chains shown by the broken curves. On the other hand, at low frequencies wedgelike shoulders appear, although those for the G'' curves are less prominent. The shoulders in the G' curves remain essentially unchanged for blends with M_{w1} below 10.5×10^3, while they extend rapidly to the lower frequency side with increasing M_{w1} for M_{w1} above 23.4×10^3.

Figure 3 shows the temperature dependence of the shift factor a_T for all the dilute blends and bulk 1-chains examined. The WLF equation[1] shown by the solid curve in the figure represents all the data very well: At the reference temperatures T_r, $f_r = 0.0644$ for all the systems. T_r for the dilute blends agreed with those for the constituent 1-chains within the experimental accuracy, because of the small w_2 in the blends. The difference in T_r (≅146, 155, and 167 °C for the blends with $10^{-3}M_{w1} = 5.2$, 10.5, and

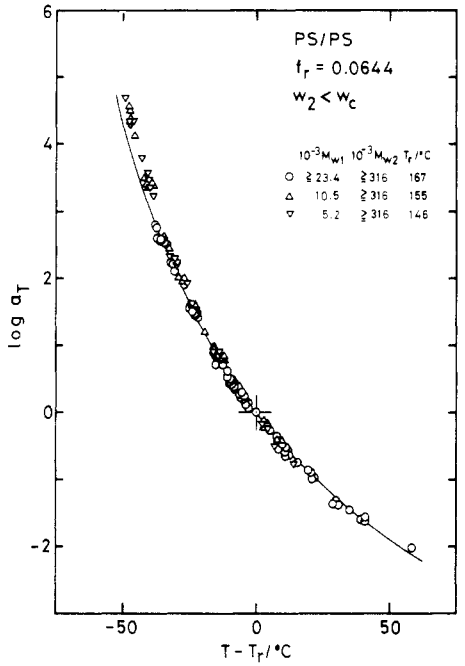

Figure 3. Temperature dependence of the shift factor a_T reduced at T_r where f_r = 0.0644. The solid curve represents the WLF equation log $a_T = -6.74(T - T_r)/(133.6 + T - T_r)$.

>23.4) corresponds to the difference in the glass transition temperatures, T_g (≅87, 95, and 107 °C, respectively, for the monodisperse PS having those M_{w1}).[27] The shift factor for the concentrated blends also exhibited the same temperature dependence when the w_2-dependent T_r was adequately chosen so that f_r = 0.0644.

Now we compare the characteristic relaxation times for dilute blends having different M_{w1} and M_{w2}. In our previous paper,[21] we analyzed the G' and G'' master curves for each blend to obtain the relaxation spectrum and evaluated the characteistic times from the location of the relevant peaks and shoulders in the spectrum. However, such a procedure should involve a little uncertainty. Thus, we made the following approach in this study.

First we introduce a blending law, eq 4,

$$H_B(\tau) = w_1H_{1B}(\tau;w_2,M_{w1},M_{w2}) + w_2H_{2B}(\tau;w_2,M_{w1},M_{w2}) \quad (4)$$

for the relaxation spectrum. In eq 4 the subscript B stands for blend. The spectra H_{1B} and H_{2B} respectively for the 1- and 2-chains in the blend should, in principle, depend on w_2, M_{w1}, and M_{w2}, which characterize the particular entanglement state in the blend. The contribution of H_{1B} and H_{2B} to H_B must be additive on a weight fraction basis. Thus, eq 4 should be applicable to any binary blend.

Generally, H_{1B} and H_{2B} cannot be replaced by $H_1(\tau)$ and $H_2(\tau)$ of the 1- and 2-chains in the bulk state. As already pointed out, however, the G' and G'' curves of the dilute blends at high frequencies are the same as those of the bulk 1-chain (cf. Figures 1 and 2). This suggests that for the dilute blends the relaxation modes of the 1-chains are the same as those in the bulk and that $H_{1B}(\tau;w_2,M_{w1},M_{w2})$ may be replaced by $H_1(\tau)$ as long as $w_2 < w_c$ and $M_{w1} << M_{w2}$.

This replacement enables us to evaluate umambiguously the characteristic relaxation time of the 2-chains as follows. First we calculate the contributions ΔA_G and $\Delta\eta_0$ of the 2-chains to the elastic coefficient and zero-shear viscosity, respectively, by

$$\Delta A_G = \omega^{-2}[G_B'(\omega) - w_1G_1'(\omega)]_{\omega\to 0} \quad (5a)$$

$$\Delta\eta_0 = \omega^{-1}[G_B''(\omega) - w_1G_1''(\omega)]_{\omega\to 0} \quad (5b)$$

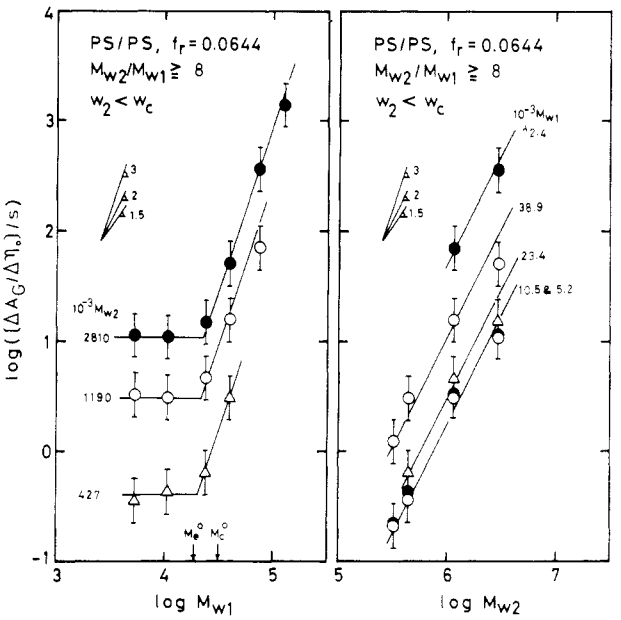

Figure 4. Dependence of $\Delta A_G/\Delta\eta_0$ at T_r of the dilute blends with the ratio $M_{w2}/M_{w1} \geq 8$ on M_{w1} and M_{w2}.

where subscript 1 stands for bulk 1-chain. The ratio $\Delta A_G/\Delta\eta_0$ is the *weight-average* relaxation time of 2-chain in the dilute blend defined by

$$\Delta A_G/\Delta\eta_0 = \int_0^\infty H_{2B}\tau\, d\tau / \int_0^\infty H_{2B}\, d\tau \quad (6)$$

Figure 4 shows the M_{w1} and M_{w2} dependence of $\Delta A_G/\Delta\eta_0$ at the iso-free-volume state with f_r = 0.0644 for the dilute blends with $M_{w2}/M_{w1} \geq 8$ including our previous data.[21,22] Both ΔA_G and $\Delta\eta_0$ were proportional to w_2, indicating that H_{2B} and $\Delta A_G/\Delta\eta_0$ are independent of w_2 for the dilute blends. The M_{w1} dependence of $\Delta A_G/\Delta\eta_0$ markedly changes with increasing M_{w1}. At large M_{w1}, $\Delta A_G/\Delta\eta_0$ is almost proportional to M_{w1}^3, but at small M_{w1}, it is independent of M_{w1}. This change is relatively sharp, and its critical molecular weight M^* (≅20 × 10^3) is very close to $M_e°$ (≅18 × 10^3) and also not far from $M_c°$ (≅31 × 10^3). On the other hand, the M_{w2} dependence of $\Delta A_G/\Delta\eta_0$ does not change and is always given by M_{w2}^2. These results are summarized as

$$\Delta A_G/\Delta\eta_0 \cong 10^{-24.7}M_{w1}^3M_{w2}^2 \quad \text{(in s)}$$
$$(M_{w2}/8 > M_{w1} > M^*;\ f_r = 0.0644) \quad (7a)$$

$$\Delta A_G/\Delta\eta_0 \cong 10^{-11.8}M_{w1}^0M_{w2}^2 \quad \text{(in s)}$$
$$(M_{w2} \gg M^* > M_{w1};\ f_r = 0.0644) \quad (7b)$$

Here it should be emphasized that the M_{w1}^3 dependence found in eq 7a appears only for the blends with the M_{w2}/M_{w1} ratio sufficiently larger than a certain value (≅8).[22] Figure 5 shows an example for L294 blends which do not exhibit the power-law type M_{w1}^3 dependence. Since M_{w2} of L294 is only by a factor of 16 larger than M^*, the range of M_{w1} where $M_{w2}/8 > M_{w1} > M^*$ is narrow so that we cannot clearly observe any power-law relation between M_{w1} and $\Delta A_G/\Delta\eta_0$. In the crossover region of $1 < M_{w2}/M_{w1} < 8$, the observed M_{w1} dependence is weaker than that described by eq 7a.

This uncertainty in the exponents for $\Delta A_G/\Delta\eta_0$ vs. M_{w1} and M_{w2} relations is also the case even for the L2580 blends having the highest M_{w2}. With increasing M_{w1} closer to M_{w2} to extend the range of M_{w1}, the power-law relation becomes unsatisfactory, since the increase in $\Delta A_G/\Delta\eta_0$ with M_{w1} becomes slower as M_{w1} approaches M_{w2} (cf. Figure 5). If the data are cast into a power-law form, the exponents

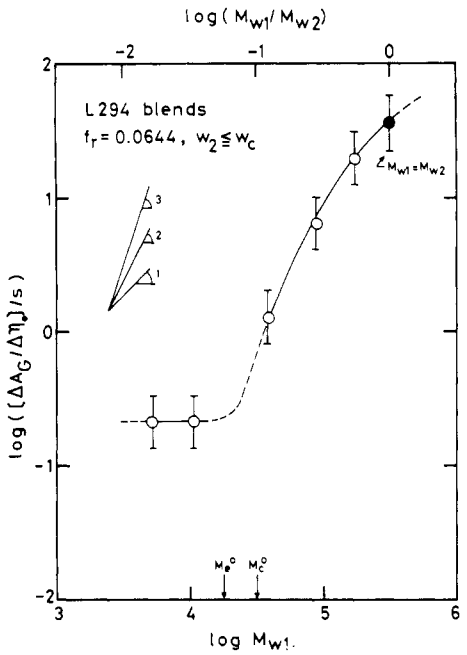

Figure 5. M_{w1} dependence of $\Delta A_G/\Delta\eta_0$ of the L294 blends at T_r where $f_r = 0.0644$.

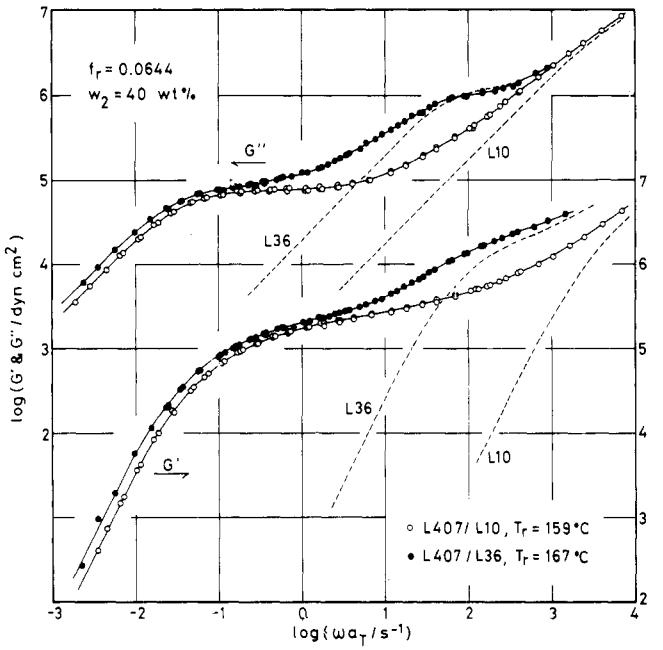

Figure 6. Master curves of the storage G' and loss G'' moduli of L407/L10 and L407/L36 blends at T_r. The L407 content w_2 is 40 wt % for both blends.

should be always smaller than the correct values. For this reason, we adopted the exponents 3 for M_{w1} and 2 for M_{w2} in eq 7a, although we may as well choose the slightly smaller values of 2.7 and 1.7, respectively, within experimental error.

Equation 7a agrees with the theoretical results for tube renewal proposed by Klein[15] and Graessley.[14] As described previously,[21] the relaxation of a 2-chain in a dilute blend with $M_{w2} \gg M_{w1} > M^*$ completes by the tube renewal.

On the other hand, eq 7b suggests that, if M_{w1} is smaller than M^*, 1-chains impose no topological constraints on 2-chains. In other words, 1-chains *do not entangle* with 2-chains but determine ζ_0 of the system. Thus, $\Delta A_G/\Delta\eta_0$ is independent of M_{w1} at the iso-free-volume state, where ζ_0 is constant. This conclusion might sound trivial, because M^* is quite close to $M_e°$ or $M_c°$, which are said to be the molecular weights characterizing the onset of entanglement. However, we point out that the molecular meaning of the onset of entanglement has not yet been stated specifically, as far as we know, but was introduced as a mere assumption. The above results on dilute blends may give a clue to understand the meaning, as discussed later.

II. Concentrated Blends. Figures 6 compares the G' and G'' data of $w_2 = 40$ wt % blends of L407/L10 (represented by open circles) and L407/L36 (filled circles) reduced at the iso-free-volume state with $f_r = 0.0644$. The broken curves in the figure represent the data for 1-chains (L10 and L36). The critical content w_c is about 10 wt % for these blends,[21] which therefore may be classified as *concentrated* blends.

As seen in Figure 6, the G' and G'' master curves for the L407/L36 and L407/L10 blends almost coincide with each other both in the low-frequency terminal zone and the rubber-to-glass transition zone at high frequencies. However, they differ appreciably with each other at intermediate frequencies in the region between 0.1 and $10^3/s^{-1}$: The L407/L36 blend exhibits a two-step rubbery plateau[1,2,21] typical of a *concentrated blend* with $M_{w2} \gg M_{w1} > M^*$, but the L407/L10 blend shows only a single-step rubbery plateau typical of a *concentrated solution* in a low molecular weight solvent. The values of G' and G'' are larger for the former than for the latter at these frequencies.

III. Contribution of 2-Chains in Concentrated Blends. Starting from eq 4, we can define the contribution ΔG^* of the 2-chains to the complex modulus G_B^* of the blend by

$$\Delta G^*(\omega) = G_B^*(\omega) - w_1 \int_{-\infty}^{\infty} H_{1B} \frac{i\omega\tau}{1 + i\omega\tau} \, d \ln \tau \quad (8)$$

For the dilute blends, H_{1B} can be replaced by H_1, and thus, the second term on the right-hand side of eq 8 by $w_1 G_1^*(\omega)$. However, for concentrated blends with $M_{w2} \gg M_{w1} > M^*$, such a replacement is not always justifiable. The wedgelike portion of the master curves corresponding to the rubber-to-glass transition is unchanged by blending, but the first-step rubbery plateau is always extended a little to the lower frequency side. (Compare the behavior of L36 and L407/L36 in the region $\omega < 10^2$ s^{-1}.)

For such a concentrated blend, H_{1B} should be divided into two portions: the short-time portion, corresponding to the transition zone, and the long-time portion, corresponding to the first-step rubbery plateau. Strictly speaking, only the former can be replaced by H_1. However, since the shift of the first plateau is usually small, we may approximate $H_{1B}(\tau;w_2,M_{w1},M_{w2})$ by $H_1(\tau/\lambda_{11})$ by introducing a small shift factor λ_{11} for the longest relaxation time of the 1-chain. Then ΔG^* becomes

$$\Delta G^*(\omega) \cong G_B^*(\omega) - w_1 G_1^*(\lambda_{11}\omega) \quad (8')$$

Figure 7 shows the contribution $\Delta G^* = \Delta G' + i\Delta G''$ of the L407 sample to G_B^* of the blends examined in Figure 6. For the L407/L10 blend, we used $\lambda_{11} = 1$ because the L10 sample did not exhibit the (first step) rubbery plateau. For the L407/L36 blend, λ_{11} was estimated to be $10^{0.1}$ to $10^{0.2}$. However, the difference in ΔG^* calculated by eq 8′ for $\lambda_{11} = 1$ and $10^{0.2}$ was negligibly small ($\leq 10^{0.05}$) in the region of interest, $\omega < 10$ s^{-1}. Thus, ΔG^* for the L407/L36 blend with $\lambda_{11} = 1$ is shown in the figure.

The behavior of a concentrated blend with $M_{w2} \gg M_{w1}$ at low frequencies is known to be similar to that of a concentrated solution of the same M_{w2} and w_2 (cf. eq 2).[1] However, at intermediate frequencies a difference may arise, because the topological interaction between the 1-

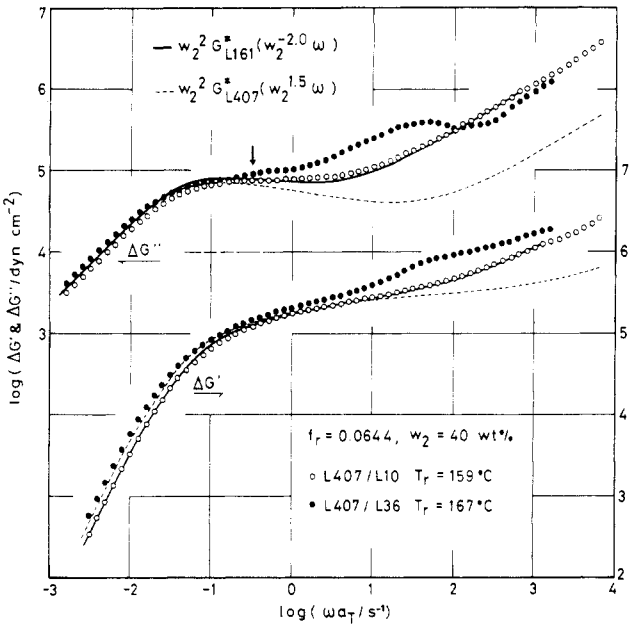

Figure 7. Frequency dependence of ΔG^* at T_r for L407/L10 and L407/L36 blends examined in Figure 6.

and 2-chains is effective only in the former. Thus, we attempted to compare ΔG^* of the blends over the entire range of frequency with those of the corresponding solutions.

The dynamic moduli G^*_{soln} of concentrated solutions of monodisperse polymers can be specified by the terminal frequencies ω^* and ω_p of the rubber-to-glass transition and rubbery plateau regions, respectively, and the height of the rubbery plateau.[1] If these parameters for a solution are compared with those of the corresponding bulk at the iso-free-volume (and hence, the iso-ζ_0) state, ω^*_{soln} of the solution is lower by a factor w_2^2 than ω^*_{bulk} of the bulk, $\omega_{p,soln}$ of the solution is higher by a factor $w_2^{-1.5}$ than $\omega_{p,bulk}$, and the rubbery plateau height of the solution is lower by a factor w_2^2 than that of the bulk as schematically shown in Figure 8a. Hence we can deduce G^*_{soln} for L407 solution with w_2 = 40 wt % by the following two alternative procedures.

In the first procedure, we employed G^*_{L407} of the bulk L407 and obtained G^*_{soln} by shifting G^*_{L407} first vertically by a factor w_2^2 and then horizontally by a factor $w_2^{-1.5}$, as schematically shown in Figure 8b (although the G'' curves are not shown). However, the resulting curves, $w_2^2 G^*_{L407}(w_2^{1.5}\omega)$, coincide with those for the solution only in the terminal zone, but not in the transition zone, since G^*_{L407} is shifted inadequately in this zone by the above procedure.

In the second procedure we employed G^*_{L161} of the bulk L161 sample. As can be seen in Table I, L161 has molecular weight $M_{w,L161} = 172 \times 10^3$, quite close to the reduced molecular weight $w_2 M_{w,L407}$ ($=171 \times 10^3$) of the L407 solution with w_2 = 40 wt %. Hence $\omega_{p,L161}$ of L161 in bulk is higher by a factor $(M_{w,L407}/M_{w,L161})^{3.5} = w_2^{-3.5}$ than that $\omega_{p,L407}$ of L407 in bulk, while the plateau moduli are the same. Thus, as illustrated in Figure 8c, we obtain G^*_{soln} by shifting G^*_{L161} first vertically by a factor w_2^2 and then horizontally by a factor w_2^2 (compare (a) and (c) in the figure). Since the G' and G'' curves in the transition zone are almost proportional to $\omega^{1/2}$,[1,2] the above procedure also gives the correct shift for the transition zone, differing from the first procedure using G^*_{L407}.

These two curves, $w_2^2 G^*_{L407}(w_2^{1.5}\omega)$ and $w_2^2 G^*_{L161}(w_2^{-2}\omega)$, are shown in Figure 7 by the thin broken and thick solid

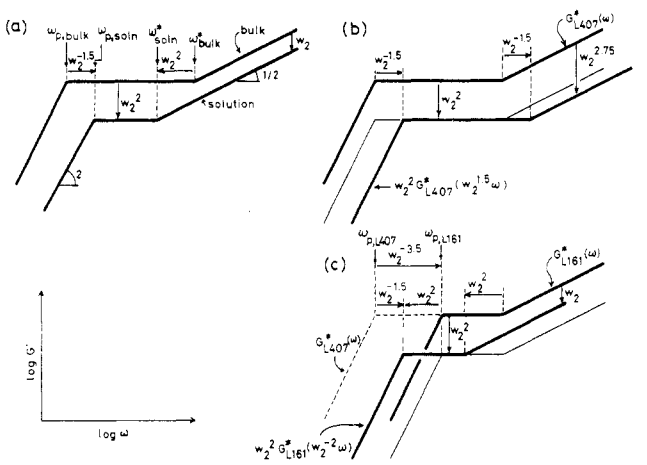

Figure 8. Schematic illustration representing the difference in the plateau height and terminal frequencies for bulk and solution samples.

curves, respectively. We notice that ΔG^* of the 40 wt % L407/L10 blend coincide with $w_2^2 G^*_{L407}(w_2^{1.5}\omega)$ only at frequencies below $10^{-0.5}$ s^{-1} but with $w_2^2 G^*_{L161}(w_2^{-2}\omega)$ over the entire frequency range examined. This result implies that the L407/L10 blend behaves as a 40 wt % solution of L407 in the L10 chains having $M_{w1} < M^*$ at any frequencies and that the L10 chains *do not entangle* with the L407 chains.

On the other hand, ΔG^* of the 40 wt % L407/L36 blend coincide with both of the calculated curves only at low frequencies. With increasing frequency, it begins to deviate even from $w_2^2 G^*_{L161}(w_2^{-2}\omega)$ and exhibits a two-step rubbery plateau. Furthermore, the lower plateau in ΔG^* is not flat but seems to contain a small maximum, which is more prominent in the $\Delta G''$ curve. The location of this small maximum corresponds to $\Delta A_G/\Delta\eta_0$ (shown by the arrow) for the dilute L407/L36 blends (cf. Figure 4).

The results for the 40 wt % L407/L36 blend may be interpreted as follows. At high frequencies, the L407 chains in the blend do not distinguish the topological constraints by the 1- and 2-chains, because the former are still effective. Thus, it exhibits a first-step rubbery plateau similar to that of L407 in bulk. In fact, this plateau was lower by a factor of w_2 (not a factor of w_2^2 expected for solutions) than that of L407 in bulk, indicating that the entanglement spacing in the first-step plateau region for the L407 chains in the blend is essentially the same as that in bulk. With further decreasing frequency, the constraints due to 1-chains become ineffective by tube renewal, leading to partial relaxation and an increase in the entanglement spacing of 2-chains. The small maximum found in Figure 7 corresponds to this process. After this process, 2-chains must escape from still-existing entanglements among themselves to relax completely.[21]

IV. Entanglements in Monodisperse Polymers. We now attempt to interpret the effect of entanglements in monodisperse flexible-chain polymer systems on the basis of the tube model, using the empirical results on the binary blends described above as a key clue.

As is well-known,[1,2] the M_w dependence of the zero-shear viscosity η_0 and steady-state compliance J_e^0 of linear monodisperse polymers shows a sharp change at the characteristic molecular weights, $M_c°$ (for η_0) and $M_c'°$ (for J_e^0). It is known that the mechanical relaxation of the polymers is strongly retarded by so-called entanglements in analogy with a bundle of flexible and long threads.

Thus, the questions to be asked are the following: What occurs at the onset of entanglements? Why do the molecular weight dependences of η_0 and J_e^0 change rather

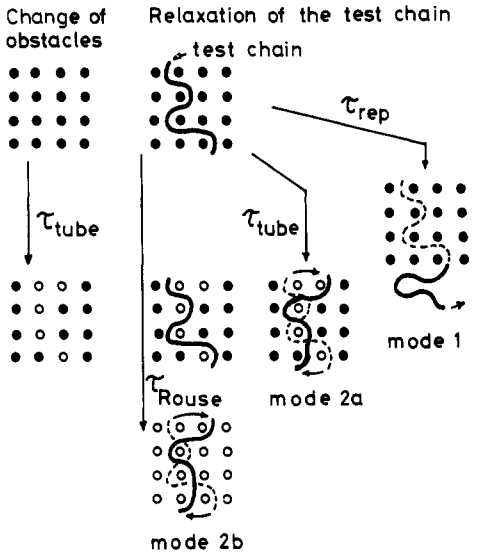

Figure 9. Schematic illustration of the possible relaxation modes in monodisperse systems. The chains (obstacles) surrounding the test chain are represented by the filled circles when they are constraining the test chain, but by the open circles when the constraints become ineffective as a result of their motion. Note that this figure *does not necessarily* imply that the inequality $\tau_{rep} < \tau_{tube} < \tau_{Rouse}$ always holds.

abruptly at $M_c°$ and $M_c'°$, despite the facts that the segment density of the polymer is essentially unchanged and the polymer coils still overlap one another at these critical molecular weights? The answer to these questions was suggested by Klein[15] by introducing the concept of tube renewal.

In condensed monodisperse polymer systems, there are at least two *potential* modes which lead to the *complete* relaxation of the chains. The characteristic times of these modes should depend on M_w. The actual relaxation modes prevail as a result of the competition between these modes.

In the framework of the tube model, one arbitrarily chooses a polymer chain in the system called the *test* chain and assumes two extreme relaxation modes: (1) *reptation*, i.e., the disengagement of the test chain from a *spatially fixed* tube; and (2) *tube renewal*, i.e., the release of constraints by *disappearance* of the tube confining the test chain. These modes are schematically illustrated in Figure 9.

The characteristic time τ_{rep} for mode 1 is given as[9-13]

$$\text{mode 1:} \qquad \tau_{rep} = K_{rep}\zeta_0 M_w^{3 \text{ or } 3.5} \tag{9}$$

where K_{rep} is a constant independent of M_w.

To define the characteristic time for mode 2, first we must evaluate the time τ_{tube} required for the change of the tube. It was given by Klein[15] and Graessley[14] as

$$\tau_{tube} = K_{tube}\zeta_0 M_w^5 \tag{10}$$

where K_{tube} is another constant independent of M_w.

The test chain has an *intrinsic* relaxation time τ_{Rouse}, determined by its M_w and ζ_0 but independent of the *topological* constraints on it:

$$\tau_{Rouse} = K_{Rouse}\zeta_0 M_w^2 \tag{11}$$

where K_{Rouse} is also a constant independent of M_w. It should be noted that τ_{Rouse} is the *shortest* relaxation time allowed for the test chain. No other mechanisms with a relaxation time shorter than τ_{Rouse} are permissible. Hence, we must classify mode 2 into two modes, modes 2a and 2b, depending on whether τ_{tube} is longer or shorter than τ_{Rouse}, respectively, as illustrated schematically in Figure 9.

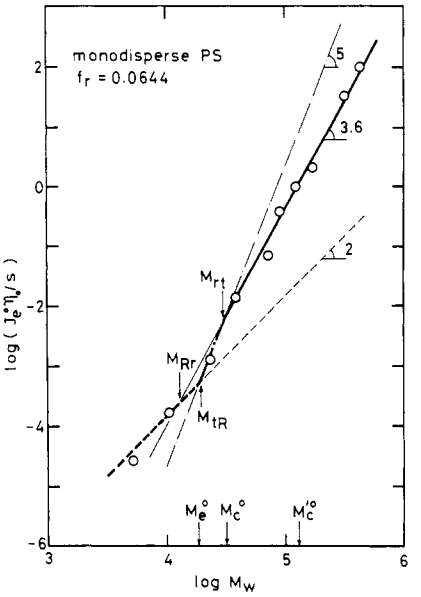

Figure 10. Comparison of the characteristic times τ_{Rouse} (broken line), τ_{rep} (solid line), and τ_{tube} (dash–dot line) and the observed weight-average times $J_e^0\eta_0$ (circles) for monodisperse PS samples. τ_{Rouse} and τ_{tube} were estimated from the data for the binary blends. All data are compared at T_r where $f_r = 0.0644$.

Mode 2a is realized for the test chain that can follow the change of the tube without delay, and thus, its characteristic time τ_{2a} is defined as

$$\text{mode 2a:} \qquad \tau_{2a} = \tau_{tube} \qquad (\text{for } \tau_{Rouse} < \tau_{tube}) \tag{12}$$

The relaxation mode often called "(constraint release by) *tube renewal*" corresponds to mode 2a. Klein[15] and Graessley[14] assumed in their theories, either explicitly or implicitly, that the test chain follows the change of the tube immediately. On the other hand, mode 2b is the mode for the test chain that cannot follow this change in the tube and has the characteristic time

$$\text{mode 2b:} \qquad \tau_{2b} = \tau_{Rouse} \qquad (\text{for } \tau_{tube} < \tau_{Rouse}) \tag{13}$$

Figure 10 compares the M_w dependence of τ_{rep} (the solid line), τ_{tube} (the dash–dot line), and τ_{Rouse} (the broken line). The relative location of the lines can be determined by the front factors of these characteristic times, and we have done so using monodisperse PS data and the binary blend data in the manner discussed later. Since these characteristic times exhibit different M_w dependences, the lines representing the reptation (1), tube renewal (2a), and Rouse (2b) modes (with subscripts r, t, and R, respectively) cross one another at different molecular weights, M_{rt}, M_{tR}, and M_{Rr}.

For system i with $M_w < M_{Rr}$, $\tau_{Rouse} > \tau_{rep} > \tau_{tube}$, and for system ii with $M_{Rr} < M_w < M_{tR}$, $\tau_{rep} > \tau_{Rouse} > \tau_{tube}$, implying that the tube does not persist for the time scale of τ_{Rouse}. For system iii with $M_{tR} < M_w < M_{rt}$, $\tau_{rep} > \tau_{tube} > \tau_{Rouse}$, implying that the tube persists for the time scale longer than τ_{Rouse} but shorter than τ_{rep}. Finally, for system iv with $M_w > M_{rt}$, $\tau_{tube} > \tau_{rep} > \tau_{Rouse}$, implying that the tube persists for the time scale longer than τ_{rep}.

In the first two cases, the test chain practically feels no constraints and must relax by its intrinsic mode 2b, because $\tau_{tube} < \tau_{Rouse}$. This was the situation we observed on the dilute blends with $M_{w1} < M^*$. On the other hand, in the last two cases, since $\tau_{Rouse} < \tau_{tube}$, the test chain feels constraints from the tube and thus must relax either by the tube renewal mode 2a in case iii or by reptation mode 1 in case iv. The former was the case we observed for dilute blends with a large M_{w2}/M_{w1} ratio but $M_{w1} > M^*$.

Hence, for monodisperse polymers, we expect that the realizable relaxation time should be τ_{Rouse} for $M_w < M_{tR}$, τ_{tube} for $M_{tR} < M_w < M_{rt}$, and τ_{rep} for $M_{rt} < M_w$, as shown by the heavy line in Figure 10.

Now we examine whether the above picture is acceptable or not, by comparing the relaxation time, $J_e^0\eta_0$, observed for the monodisperse PS samples with the expected τ_{tube}, τ_{rep}, and τ_{Rouse} lines. We have already observed the tube renewal mode 2a for the binary blends. Thus, the τ_{tube} line was drawn in Figure 10 by substituting $M_{w1} = M_{w2} = M_w$ in the *empirically determined* eq 7a. Likewise, the τ_{Rouse} line was drawn by using eq 7b for the mode 2b in the binary blends.

In Figure 10, we first notice that the $J_e^0\eta_0$ data points (circles) for the monodisperse PS samples with $M_w \gg M^*$ ($=M_{tR}$ in the above notation) fall between the τ_{Rouse} (broken) and τ_{tube} (dash–dot) lines. Thus, as a first approximation, we may assume that the tubes are fixed in space until the actual polymer chains with $M_w \gg M^*$ complete the relaxation essentially by reptation. We may cast the $J_e^0\eta_0$ data shown in Figure 10 for the PS samples with $M_w > M_c'^\circ$ (the so-called fully entangled state) equal to τ_{rep} as

$$\tau_{rep} = J_e^0\eta_0 \cong 5 \times 10^{-19} M_w^{3.6} \text{ (in s)} \quad (M_w > M_c'^\circ;\ f_r = 0.0644) \quad (14)$$

By extrapolating eq 14 to small M_w, we can locate M_{rt} and M_{tR} for the PS samples, as the intersections of the solid, dash–dot, and broken lines. They are interestingly enough very close to M_c° and M_e° of the PS samples, respectively.

As can be seen in Figure 10, the data points for the PS samples follow the heavy line. However, the range of M_w satisfying $M_{tR} < M_w < M_{rt}$ is so narrow that we hardly observe the pure mode 2a taking place. This means that as soon as τ_{tube} exceeds τ_{Rouse} of the chain with increasing M_w above M^*, τ_{tube} also exceeds τ_{rep}. In other words, the tube becomes practically fixed in space. Hence, we may say that the onset of entanglements in a monodisperse polymer corresponds to the change of the relaxation mode from the Rouse 2b mode to the reptation 1 mode. The essential point is that this change of the relaxation mode takes place as a result of the competition between the tube renewal and the intrinsic mode.

At this point, we should also note that the difference between the observed $J_e^0\eta_0$ and τ_{tube} is not very large, especially in the crossover region slightly above M^*. Even at M_w as high as 300×10^3, τ_{tube} is larger only by a factor of 10 than τ_{rep} or $J_e^0\eta_0$. Thus, although the tube theory implicitly assumes that the modes 1 and 2a do not occur simultaneously,[28] the actual relaxation mode may contain a contribution of the tube renewal mode to some extent even in this high-M_w region. This speculation may be supported by the fact that linear free chains trapped in a cross-linked rubber network have a longer relaxation time than that in the un-cross-linked bulk state.[29]

Finally, we must admit that the above interpretation of the onset of entanglements still has not answered the question why M_e° is 18×10^3 for PS but 2×10^3 for polybutadiene.[1,2] The value of M_e° was determined by the position where eq 9, 10, and 11 cross one another and hence by the values of prefactors K_{rep}, K_{tube}, and K_{Rouse}. The chemical properties of the polymers, the dimension and the segment concentration of the polymer coils, etc. should determine the prefactors and the value of M_e° (or M_c°) of the individual polymers.[24,25] These are questions still to be answered.

Acknowledgment. We thank Dr. Mitsutoshi Fukuda, Toyo Soda Mfg. Co. Ltd., for supplying us with most of the PS samples used in this study.

Registry No. PS (homopolymer), 9003-53-6.

References and Notes

(1) Ferry, J. D. "Viscoelastic Properties of Polymers", 3rd ed.; Wiley, New York, 1980.
(2) Graessley, W. W. *Adv. Polym. Sci.* **1974**, *16*.
(3) Graessley, W. W.; Masuda, T.; Roovers, J.; Hadjichristidis, N. *Macromolecules* **1976**, *9*, 127.
(4) Graessley, W. W.; Roovers, J. *Macromolecules* **1979**, *12*, 959.
(5) Raju, V. R.; Menezes, E. V.; Marin, G.; Graessley, W. W.; Fetters, L. J. *Macromolecules* **1981**, *14*, 1668.
(6) Masuda, T.; Ohta, Y.; Onogi, S. *Macromolecules* **1971**, *4*, 763.
(7) Kajiura, H.; Ushiyama, Y.; Fujita, T.; Nagasawa, M. *Macromolecules* **1978**, *1*, 894.
(8) Roovers, J. *Macromolecules* **1984**, *17*, 1196.
(9) de Gennes, P.-G. *J. Chem. Phys.* **1971**, *55*, 572.
(10) de Gennes, P.-G. "Scaling Concepts in Polymer Physics"; Cornell University Press: Ithaca, NY, 1979.
(11) Doi, M.; Edwards, S. F. *J. Chem. Soc., Faraday Trans. 2* **1978**, *74*, 1789, 1802, 1818; **1979**, *75*, 38.
(12) Doi, M. *J. Polym. Sci., Polym. Phys. Ed.* **1980**, *18*, 1005, 1981.
(13) Doi, M. *J. Polym. Sci., Polym. Phys. Ed.* **1983**, *21*, 667.
(14) Graessley, W. W. *Adv. Polym. Sci.* **1982**, *47*.
(15) Klein, J. *Macromolecules* **1978**, *11*, 852.
(16) Doi, M.; Kuzuu, N. *J. Polym. Sci., Polym. Lett. Ed.* **1980**, *18*, 775.
(17) Pearson, D. S.; Helfand, E. *Macromolecules* **1984**, *17*, 888.
(18) Watanabe, H.; Kotaka, T. *Macromolecules* **1983**, *16*, 769; **1984**, *17*, 342.
(19) Graessley, W. W. *J. Polym. Sci., Polym. Phys. Ed.* **1980**, *18*, 27.
(20) Kurata, M. *Macromolecules* **1984**, *17*, 895.
(21) Watanabe, H.; Kotaka, T. *Macromolecules* **1984**, *17*, 2316.
(22) Watanabe, H.; Sakamoto, T.; Kotaka, T. *Macromolecules* **1985**, *18*, 1008.
(23) Montfort, J. P.; Marin, G.; Monge, P. *Macromolecules* **1984**, *17*, 1551.
(24) Fox, T. G.; Allen, V. R. *J. Chem. Phys.* **1964**, *41*, 344. See also: Berry, G. C.; Fox, T. G. *Adv. Polym. Sci.* **1968**, *5*.
(25) Graessley, W. W.; Edwards, S. F. *Polymer* **1981**, *22*, 1329.
(26) Markovitz, H. *J. Appl. Phys.* **1952**, *23*, 1070.
(27) Kudose, I. M.S. Dissertation, Osaka Unversity, 1983. Kudose, I.; Kotaka, T. *Macromolecules* **1984**, *17*, 2325.
(28) An approximate characteristic time of the mixed mode may be evaluated by taking an adequate average of τ_{rep} and τ_{tube}, as shown by Klein[15] and Graessley.[14] However, for the exact evalution of the mixed mode, the cooperative modes of reptation and tube renewal must be taken into account.
(29) Kan, H.-C.; Ferry, J. D.; Fetters, L. J. *Macromolecules* **1980**, *13*, 1571. Taylor, C. R.; Kan, H.-C.; Nelb, G. W.; Ferry, J. D. *J. Rheol.* **1981**, *25*, 507.